Journal of
Nanoscience and Nanotechnology
Vol. 8, 3774–3780, 2008

Stiffness and Thickness of Boron-Nitride Nanotubes

J. Song[1], J. Wu[2], Y. Huang[3,*], K. C. Hwang[2], and H. Jiang[4]

[1]*Department of Mechanical Science and Engineering, University of Illinois, Urbana, IL 61801, USA*
[2]*FML, Department of Engineering Mechanics, Tsinghua University, Beijing 10084, China*
[3]*Department of Civil and Environmental Engineering and Department of Mechanical Engineering, Northwestern University, Evanston, IL 60208, USA*
[4]*Department of Mechanical and Aerospace Engineering, Arizona State University, Tempe, AZ 85287, USA*

We establish an analytic approach to determine the tensile and bending stiffness of a hexagonal boron-nitride (h-BN) monolayer and single- and multi-wall boron-nitride nanotubes (BNNTs) directly from the interatomic potential. Such an approach enables one to bypass atomistic simulations and to give the tensile and bending stiffness in terms of the parameters in the potential. For single- and multi-wall BNNTs, the stiffness also depends on the (inner most or outer most) wall radius and the number of the walls. The thickness of h-BN monolayer is also discussed.

Keywords: Boron-Nitride Nanotube, Bending Stiffness, Interatomic Potential, Analytic Expression.

RESEARCH ARTICLE

1. INTRODUCTION

Boron-nitride nanotubes (BNNTs) possess unique structural, mechanical, thermal, electrical and chemical properties, and represent an important class of nanotubes. The tensile stiffness of BNNTs[1–3] is comparable to that of carbon nanotubes. The thermal conductivity along the nanotube is very high.[4] However, contrary to carbon nanotubes, BNNTs always have large band gaps regardless of the chirality and diameter,[5] and are therefore semiconductors. They also have good resistance to oxidation at high temperature.[6]

There are limited experimental[7,8] and atomistic studies[1–3,9–14] of BNNT mechanical properties. Song et al.[15] established a continuum theory for BNNTs from the interatomic potential for boron nitride.[16,17] The tensile stiffness given by this atomistic-based continuum theory agrees well with the atomistic simulation results. However, both atomistic and continuum studies can determine the BNNT stiffness Eh only, which is the product of Young's modulus E and BNNT thickness h. One needs to assume a thickness h in order to determine its Young's modulus, even though it is ambiguous to define the thickness for a single layer of atoms. One assumption is to take the interlayer spacing of hexagonal boron nitride (h-BN) $h =$ 0.34 nm as the BNNT thickness.[1,9,11,15]

Yakobson et al.[18] adopted a different approach to determine the Young's modulus and thickness of single-wall carbon nanotubes by modeling them as linear elastic thin shells and fitting them to the atomistic simulation results of tensile stiffness Eh and bending stiffness $Eh^3/12$. Such an approach gives much smaller carbon nanotube thickness from 0.06 to 0.09 nm, depending on the interatomic potential and simulation details.

Huang et al.[19] established an *analytic* method that bypasses atomistic simulations to determine the tensile and bending stiffness of a single layer of carbon atoms (i.e., graphene) directly from the interatomic potential. Analytical expressions of tensile and bending stiffness of graphene are obtained in terms of parameters in the interatomic potential. Its bending stiffness clearly results from the multi-body atomistic interaction in carbon, i.e., a pair potential would give a vanishing bending stiffness. Furthermore, the thickness defined from the tensile and bending stiffness[18] is not strictly a constant for each interatomic potential since it depends on the stress state (e.g., uniaxial tension, uniaxial stretching, biaxial stretching).

The purpose of this paper is to extend Huang et al.'s[19] approach and study the BNNT tensile and bending stiffness. The formulation of multi-body interatomic potential for boron nitride is given in Section 2. This potential has been used to study BNNT and hexagonal boron nitride (h-BN),[13–15,17,20–22] and the latter can be viewed as a BNNT unfolded to planes of boron and nitrogen atoms. The tensile and bending stiffness of an h-BN monolayer are given analytically in Section 3 in terms of parameters in the interatomic potential. The thickness of h-BN monolayer is studied in Section 4. The results for BNNTs are given in Section 5, in which the bending stiffness associated with a BNNT wall and that associated with a BNNT tube are clearly distinguished.

*Author to whom correspondence should be addressed.

1533-4880/2008/8/3774/007 doi:10.1166/jnn.2008.015

2. FORMULATION OF MULTI-BODY INTERATOMIC POTENTIAL FOR BORON NITRIDE

The interatomic potential for boron nitride can be generally written as

$$V = V(r_{ij}; \theta_{ijk}, k \neq i, j) = V(r_{ij}; \cos\theta_{ijk}, k \neq i, j) \quad (1)$$

for boron and nitrogen atoms i and j, where r_{ij} is the bond length, θ_{ijk} is the bond angle between i—j and i—k bonds, and k ($\neq i,j$) represents atoms in the vicinity. The θ_{ijk} term, or equivalently, $\cos\theta_{ijk}$ term represents the multi-body atomistic interactions in boron nitride. For the unstrained, equilibrium state (i.e., strain $\varepsilon = 0$), the equilibrium bond length and angle are denoted by $(r_{ij})_0$ and $(\cos\theta_{ijk})_0$, respectively.

For an infinitesimal strain ε, the changes of bond length $r_{ij} - (r_{ij})_0$ and bond angle $\theta_{ijk} - (\theta_{ijk})_0$ are also infinitesimal such that the interatomic potential in (1) can be expanded to the Taylor series. We use an h-BN monolayer (a layer of boron and nitrogen atoms) shown in Figure 1 to illustrate this, where the solid and open circles represent the boron and nitrogen atoms, respectively. The unit cell containing a boron atom and a nitrogen atom is shown by the shaded area. The bond angle for h-BN at the unstrained, equilibrium state is $(\theta_{ijk})_0 = 120°$. The equilibrium length r_0 of boron-nitrogen bond is to be determined by minimizing the potential V at the fixed bond angle 120°, i.e.,

$$\left.\frac{\partial V}{\partial r_{ij}}\right|_{r_{ij}=r_0, \theta_{ijk}=120°} = 0 \quad (2)$$

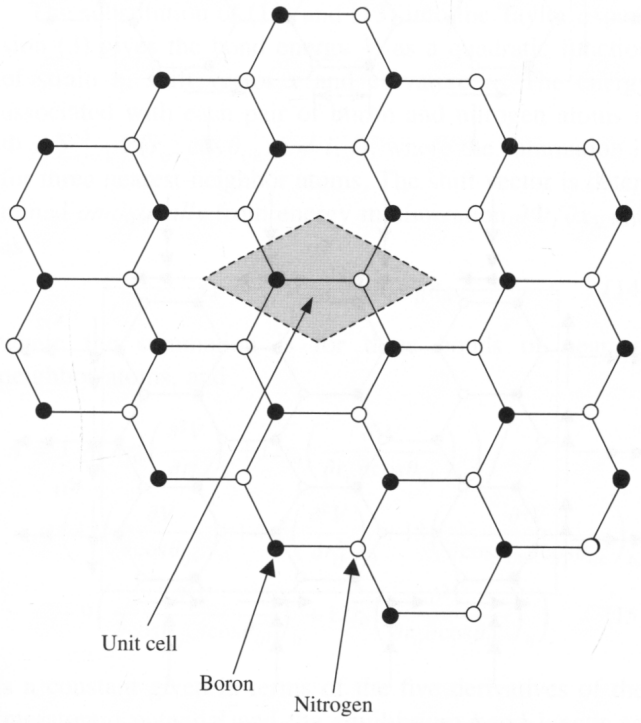

Fig. 1. A unit cell for a hexagonal boron-nitride monolayer.

For an infinitesimal strain ε, $r_{ij} - r_0$ and $\cos\theta_{ijk} + 1/2$ are also infinitesimal. The Taylor expansion of (1) for the h-BN monolayer is

$$\begin{aligned} V = V_0 &+ \sum_{k\neq i,j}\left(\frac{\partial V}{\partial \cos\theta_{ijk}}\right)_0\left(\cos\theta_{ijk} + \frac{1}{2}\right) + \frac{1}{2}\left(\frac{\partial^2 V}{\partial r_{ij}^2}\right)_0 \\ &\times (r_{ij} - r_0)^2 + \sum_{k\neq i,j}\left(\frac{\partial^2 V}{\partial r_{ij}\partial\cos\theta_{ijk}}\right)_0 (r_{ij} - r_0) \\ &\times\left(\cos\theta_{ijk} + \frac{1}{2}\right) + \frac{1}{2}\sum_{k,l\neq i,j}\left(\frac{\partial^2 V}{\partial\cos\theta_{ijk}\partial\cos\theta_{ijl}}\right)_0 \\ &\times\left(\cos\theta_{ijk} + \frac{1}{2}\right)\left(\cos\theta_{ijl} + \frac{1}{2}\right) \end{aligned} \quad (3)$$

where the subscript "0" denotes the values at the unstrained, equilibrium state, $r_{ij} = r_0$ and $\theta_{ijk} = 120°$; and the terms higher than the second order are neglected since they do not contribute to the tensile and bending stiffness which are defined at the infinitesimal strain. Equation (3) holds for both boron and nitrogen atoms at the unstrained, equilibrium state since all bond lengths are the same, and all bond angles equal to 120°. It involves five constants of the interatomic potential, namely the first-order derivative $(\partial V/\partial\cos\theta_{ijk})_0$, and second-order derivatives $(\partial^2 V/\partial r_{ij}^2)_0$, $(\partial^2 V/\partial r_{ij}\partial\cos\theta_{ijk})_0$, $(\partial^2 V/\partial\cos\theta_{ijk}\partial\cos\theta_{ijk})_0$, and $(\partial^2 V/\partial\cos\theta_{ijk}\partial\cos\theta_{ijl})_0$ $(k \neq l)$. These five constants at the unstrained, equilibrium state ($\varepsilon = 0$) can be *analytically* obtained for any interatomic potential. The tensile, bending stiffness and thickness of h-BN monolayer will be given in terms of these five constants in Sections 3 and 4.

An example of the interatomic potential for boron nitride[16] is in the form of the Tersoff formulism

$$V(r_{ij}; \cos\theta_{ijk}) = V_R(r_{ij}) - B_{ij}V_A(r_{ij}) \quad (4)$$

where V_R and V_A are the repulsive and attractive pair terms (depending only on r_{ij}) given by

$$\begin{aligned} V_R(r) &= \frac{D_0}{S-1}\exp[-\beta\sqrt{2S}(r - r_0^*)]\cdot f_C(r) \\ V_A(r) &= \frac{SD_0}{S-1}\exp[-\beta\sqrt{2/S}(r - r_0^*)]\cdot f_C(r) \end{aligned} \quad (5)$$

D_0 and r_0^* are the dimmer energy and separation, respectively, given in Table I together with constants S and β. These constants depend on the index pair (boron–nitrogen, nitrogen–nitrogen, and boron–boron). The cutoff function f_C in (5) limits the interaction shell on the next neighbors inside the radius R, and is given by

$$f_C(r) = \begin{cases} 1 & r \leq R - D \\ \dfrac{1}{2} - \dfrac{1}{2}\dfrac{\sin[\pi(r-R)}{(2D)]} & |r - R| \leq D \\ 0 & r \geq R + D \end{cases} \quad (6)$$

RESEARCH ARTICLE

Table I. Parameters in the boron-nitride interatomic potential.

	BN-interaction	NN-interaction	BB-interaction
D_0 (eV)	6.36	9.91	3.08
r_0^* (Å)	1.33	1.11	1.59
S	1.0769	1.0769	1.0769
β (Å^{-1})	2.043057	1.92787	1.5244506
R (Å)	2.0	2.0	2.0
D (Å)	0.1	0.1	0.1
n	0.364153367	0.6184432	3.9929061
γ	0.000011134	0.019251	0.0000016
λ (Å^{-1})	1.9925	0	0
c	1092.9287	17.7959	0.52629
d	12.38	5.9484	0.001587
h^*	−0.5413	0	0.5

Source: Reprinted with permission from [16], K. Albe et al., *Radiat. Eff. Defects Solids* 141, 85 (**1997a**). © 1997, Taylor and Francis Ltd.

where $R = 2$ Å and $D = 0.1$ Å for all index pairs (i.e., boron–nitrogen, nitrogen–nitrogen and boron–boron) as shown in Table I. The multi-body coupling term B_{ij} in (4) results from the interaction between atoms i, j and their local environment, and is given by

$$B_{ij} = (1+\gamma^n \chi_{ij}^n)^{\frac{-1}{2n}}$$
$$\chi_{ij} = \sum_{k\neq i,j} G(\theta_{ijk}) f_C(r_{ik}) \exp[\lambda^3 (r_{ij} - r_{ik})^3] \quad (7)$$
$$G(\theta_{ijk}) = 1 + \frac{c^2}{d^2} - \frac{c^2}{d^2 + (h^* - \cos\theta_{ijk})^2}$$

where k denotes atoms other than i and j, θ_{ijk} is the angle between bonds i—j and i—k, and the constants n, γ, λ, c, d and h^* depend on the index pair as shown in Table I.

The equilibrium bond length r_0 can be solved *analytically* from (2) as

$$r_0 = r_0^* - \frac{1}{\beta}\frac{\sqrt{S/2}}{(S-1)} \ln B_0 \quad (8)$$

where B_0 is the multi-body coupling term B_{ij} in (7) evaluated at $\theta_{ijk} = 120°$, and is given by

$$B_0 = [1 + (2\gamma G_0)^n]^{\frac{-1}{2n}} \quad (9)$$

and G_0 is the function G in (7) evaluated at $\theta_{ijk} = 120°$,

$$G_0 = 1 + \frac{c^2}{d^2} - \frac{c^2}{d^2 + (h^* + 1/2)^2} \quad (10)$$

For the constants given in Table I, $G_0 = 1.09$, $B_0 = 0.97$, and the equilibrium bond length $r_0 = 0.146$ nm. The other first-order derivative can also be obtained *analytically* as

$$\left(\frac{\partial V}{\partial \cos\theta_{ijk}}\right)_0 = -\frac{SD_0}{S-1}\gamma c^2 \frac{(h^* + 1/2)}{[d^2 + (h^* + 1/2)^2]^2} \times (2\gamma G_0)^{n-1} B_0^{2n + \frac{S}{S-1}} \quad (11)$$

which gives $(\partial V/\partial \cos\theta_{ijk})_0 = 1.18$ eV, and it reflects the multi-body atomistic interactions. The *analytical* expressions of the second-order derivatives are given in the appendix, which give $(\partial^2 V/\partial r_{ij}^2)_0 = 3570.84$ eV/nm^2, $(\partial^2 V/\partial r_{ij}\partial \cos\theta_{ijk})_0 = -32.91$ eV/nm, $(\partial^2 V/\partial \cos\theta_{ijk}\partial \cos\theta_{ijk})_0 = 27.12$ eV, and $(\partial^2 V/\partial \cos\theta_{ijk}\partial \cos\theta_{ijl})_0$ $(k \neq l) = -1.49$ eV.

3. TENSILE AND BENDING STIFFNESS OF A HEXAGONAL BORON-NITRIDE MONOLAYER

We first study an h-BN monolayer subject to uniform in-plane normal strains ε_{11} and ε_{22} and shear strain ε_{12}, as shown in Figure 2(a). The atom positions are nonuniform even for a uniform strain because the h-BN monolayer does not have a simple Bravais lattice. The h-BN monolayer is decomposed to a simple Bravais sub-lattice of boron atoms (solid circles) and another of nitrogen atoms (open circles) as shown in Figure 2(a). A shift vector between two sub-lattices is introduced to ensure equilibrium of atoms via energy minimization.[19, 23, 24] The distance r_{ij} between the boron and nitrogen is given by

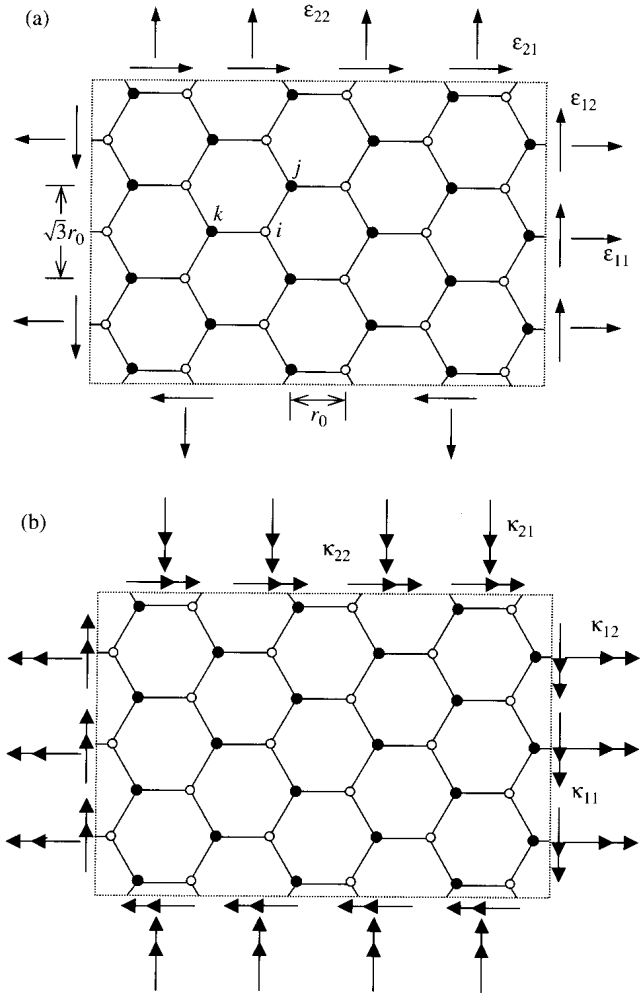

Fig. 2. A schematic diagram of a hexagonal boron-nitride monolayer subject to (a) in-plane strain and (b) curvature.

RESEARCH ARTICLE

$r_{ij}^2 = r_0^2(\delta_{\alpha\beta}+2\varepsilon_{\alpha\beta})(n_\alpha+x_\alpha)(n_\beta+x_\beta)$, where r_0 and $\boldsymbol{n}$ are the bond length and bond direction prior to deformation, $\delta_{\alpha\beta}$ is the second-order identity tensor, and $\boldsymbol{x}=\boldsymbol{x}(\varepsilon)$ is the shift vector (normalized by r_0) to be determined *analytically* via energy minimization.

We now consider the h-BN monolayer subject to combined in-plane strain $\varepsilon_{\alpha\beta}$ $(\alpha,\beta=1,2)$ and curvature κ_{11}, κ_{22} and κ_{12} (Fig. 2), which cause stretching and bending of the h-BN monolayer, respectively. The distance between the boron and nitrogen atoms now becomes

$$r_{ij}^2 = r_0^2(\delta_{\alpha\beta}+2\varepsilon_{\alpha\beta})(n_\alpha+x_\alpha)(n_\beta+x_\beta) - r_0^4[\kappa_{\alpha\beta}(n_\alpha+x_\alpha)(n_\beta+x_\beta)]^2/12 \quad (12)$$

where the first term on the right hand side is due to the in-plane strain, the second term represents the bond length reduction due to the curvature, and the shift vector $\boldsymbol{x}=\boldsymbol{x}(\varepsilon,\boldsymbol{\kappa})$ is to be determined *analytically* via energy minimization. The bond angle θ_{ijk} between bonds i—j and i—k can be similarly obtained as

$$\cos\theta_{ijk} = \frac{r_0^2}{r_{ij}r_{ik}}(n_\alpha^{(1)}+x_\alpha)(n_\lambda^{(2)}+x_\lambda) \times\left\{\delta_{\alpha\lambda}+2\varepsilon_{\alpha\lambda}+\frac{r_0^2}{12}\kappa_{\alpha\beta}\kappa_{\gamma\lambda}\times[3(n_\beta^{(1)}+x_\beta) \times(n_\gamma^{(2)}+x_\gamma)-2(n_\beta^{(2)}+x_\beta)(n_\gamma^{(2)}+x_\gamma) -2(n_\beta^{(1)}+x_\beta)(n_\gamma^{(1)}+x_\gamma)]\right\} \quad (13)$$

where $\boldsymbol{n}^{(1)}$ and $\boldsymbol{n}^{(2)}$ represent the directions of i—j and i—k bonds prior to deformation, respectively.

The substitution of (12) and (13) into the Taylor expansion (3) gives the bond energy V as a quadratic function of strain ε, shift vector $\boldsymbol{x}$ and curvature $\boldsymbol{\kappa}$. The energy associated with each pair of boron and nitrogen atoms is $\Phi=\sum_{j=1}^{3}V(r_{ij};\cos\theta_{ijk},k\neq i,j)$, where the summation is for three nearest-neighbor atoms. The shift vector is determined *analytically* from energy minimization $\partial\Phi/\partial x_\lambda=0$ as

$$x_\lambda = \frac{2}{3}A\varepsilon_{\alpha\beta}\sum n_\alpha n_\beta n_\lambda \quad (14)$$

where the summation is for three bonds of nearest-neighbor atoms, and

$$A = 1-\left(8r_0^2\left(\frac{\partial^2V}{\partial r_{ij}^2}\right)_0+12r_0\left(\frac{\partial^2V}{\partial r_{ij}\partial\cos\theta_{ijk}}\right)_0\right)\Big/ \left(12\left(\frac{\partial V}{\partial\cos\theta_{ijk}}\right)_0+4r_0^2\left(\frac{\partial^2V}{\partial r_{ij}^2}\right)_0+18\left(\frac{\partial^2V}{\partial\cos\theta_{ijk}\partial\cos\theta_{ijk}}\right)_0 -9\left(\frac{\partial^2V}{\partial\cos\theta_{ijk}\partial\cos\theta_{ijl}}\right)_0+12r_0\left(\frac{\partial^2V}{\partial r_{ij}\partial\cos\theta_{ijk}}\right)_0\right) \quad (15)$$

is a constant given in terms of the five derivatives of the interatomic potential and the equilibrium bond length r_0. The shift vector in (14) depends on the in-plane strain ε but not curvature $\boldsymbol{\kappa}$. In fact, it depends only on the deviatoric strain $\varepsilon_{\alpha\beta}=\varepsilon_{\alpha\beta}-(\varepsilon_{11}+\varepsilon_{22})\delta_{\alpha\beta}/2$ since the equi-biaxial strain $\varepsilon_{\alpha\beta}=\varepsilon\delta_{\alpha\beta}$ gives a vanishing shift vector $x_\lambda=0$.

The strain energy density (energy per unit area of the h-BN monolayer) is $\Phi/(3\sqrt{3}r_0^2/2)$, where $3\sqrt{3}r_0^2/2$ is the area of the unit cell in Figure 1. The strain energy density becomes a quadratic function of ε and $\boldsymbol{\kappa}$ once the shift vector $\boldsymbol{x}$ is substituted by (14). The derivative of the strain energy density with respect to ε gives the stress

$$(\sigma_{11}+\sigma_{22})h = \frac{1}{\sqrt{3}}\left(\frac{\partial^2V}{\partial r_{ij}^2}\right)_0(\varepsilon_{11}+\varepsilon_{22}) \quad \begin{Bmatrix}(\sigma_{11}-\sigma_{22})h\\ \sigma_{12}h\end{Bmatrix} = \frac{B}{8\sqrt{3}}\begin{Bmatrix}\varepsilon_{11}-\varepsilon_{22}\\ \varepsilon_{12}\end{Bmatrix} \quad (16)$$

where the stress appears together with the "thickness" h of the h-BN monolayer since the strain energy density is the energy per unit area (instead of volume), and

$$B = \frac{3(1-A)^2}{r_0^2}\left[4\left(\frac{\partial V}{\partial\cos\theta_{ijk}}\right)_0+6\left(\frac{\partial^2V}{\partial\cos\theta_{ijk}\partial\cos\theta_{ijk}}\right)_0 -3\left(\frac{\partial^2V}{\partial\cos\theta_{ijk}\partial\cos\theta_{ijl}}\right)_0\right]+4(1+A)^2\left(\frac{\partial^2V}{\partial r_{ij}^2}\right)_0 -12\frac{(1-A^2)}{r_0}\left(\frac{\partial^2V}{\partial r_{ij}\partial\cos\theta_{ijk}}\right)_0 \quad (17)$$

The tensile stiffness Eh of the h-BN monolayer is the ratio of $\sigma_{11}h/\varepsilon_{11}$ for uniaxial tension $\sigma_{11}\neq0$ and $\sigma_{22}=0$, and is given *analytically* by

$$Eh = \frac{B}{4\sqrt{3}}\frac{\left(\frac{\partial^2V}{\partial r_{ij}^2}\right)_0}{\left(\frac{\partial^2V}{\partial r_{ij}^2}\right)_0+\frac{B}{8}} \quad (18)$$

For Albe et al.'s[16] potential, the tensile stiffness is $Eh=2364.21$ eV/nm^2. The in-plane shear stiffness $\sigma_{12}h/(2\varepsilon_{12})$ is $\mu_{\text{in-plane}}h=B/(16\sqrt{3})$, where $\mu_{\text{in-plane}}$ represents the equivalent in-plane shear modulus.

The derivative of strain energy density with respect to the curvature $\boldsymbol{\kappa}$ gives the bending moment,

$$M_{11}+M_{22} = \frac{\sqrt{3}}{2}\left(\frac{\partial V}{\partial\cos\theta_{ijk}}\right)_0(\kappa_{11}+\kappa_{22}) \quad \begin{Bmatrix}M_{11}-M_{22}\\ M_{12}\end{Bmatrix}=0 \quad (19)$$

The biaxial bending stiffness (ratio of $M_{11}+M_{22}$ to $\kappa_{11}+\kappa_{22}$) is $\sqrt{3}(\partial V/\partial\cos\theta_{ijk})_0/2$, which reflects the multi-body atomistic interactions, and equals to 1.02 eV for Albe et al.'s[16] potential. The h-BN monolayer cannot be subject to any torsion (since $M_{12}=0$), and the bending moment is equi-biaxial, $M_{11}=M_{22}$, regardless of the curvature. Similar observations have been made for graphene.[19]

4. THICKNESS OF THE h-BN MONOLAYER

The moment–curvature relation for a thin layer of continuum solid[25] with thickness h is $M_{11}+M_{22}=Eh^3(\kappa_{11}+\kappa_{22})/[12(1-\nu)]$, $M_{11}-M_{22}=Eh^3(\kappa_{11}-\kappa_{22})/[12(1+\nu)]$ and $M_{12}=Eh^3\kappa_{12}/[12(1+\nu)]$. The in-plane stress–strain relation is $\sigma_{11}+\sigma_{22}=E(\varepsilon_{11}+\varepsilon_{22})/(1-\nu)$, $\sigma_{11}-\sigma_{22}=E(\varepsilon_{11}-\varepsilon_{22})/(1+\nu)$ and $\sigma_{12}=E\varepsilon_{12}/(1+\nu)$. Therefore, the ratio of bending stiffness to tensile stiffness is always $h^2/12$ for different loadings, including

(i) the ratio of biaxial bending stiffness $(M_{11}+M_{22})/(\kappa_{11}+\kappa_{22})=Eh^3/[12(1-\nu)]$ to biaxial tensile stiffness $(\sigma_{11}+\sigma_{22})h/(\varepsilon_{11}+\varepsilon_{22})=Eh/(1-\nu)$;

(ii) the ratio of uniaxial bending stiffness $M_{11}/\kappa_{11}=Eh^3/12$ $(M_{22}=0)$ to uniaxial tensile stiffness $\sigma_{11}h/\varepsilon_{11}=Eh$ $(\sigma_{22}=0)$, and

(iii) the ratio of torsion stiffness $M_{12}/(2\kappa_{12})=Eh^3/[24(1+\nu)]$ to shear stiffness $\sigma_{12}h/(2\varepsilon_{12})=Eh/[2(1+\nu)]$.

Based on the above observations, Yakobson et al.[18] defined the thickness of single-wall carbon nanotubes from the ratio of bending stiffness to tensile stiffness,

$$h=\sqrt{\frac{12*\text{bending stiffness}}{\text{tension stiffness}}} \tag{20}$$

Such a thickness, however, may not be well defined for the h-BN monolayer. For example, the ratio of biaxial bending stiffness in (19) to biaxial tensile stiffness in (16) gives

$$h_{\text{biaxial}}=3\sqrt{\frac{2\left(\frac{\partial V}{\partial\cos\theta_{ijk}}\right)_0}{\left(\frac{\partial^2 V}{\partial r_{ij}^2}\right)_0}} \tag{21}$$

but the ratio of torsion stiffness in (19) to shear stiffness (16) gives a vanishing thickness

$$h_{\text{shear}}=0 \tag{22}$$

Furthermore, the uniaxial bending stiffness cannot even be defined since M_{22} always equals to M_{11} from (19) for an h-BN monolayer, i.e., it cannot be subject to uniaxial bending $M_{22}=0$. Therefore, the thickness defined by (20) is not a constant and depends on the type of loading. Huang et al.[19] made similar observations for the graphene, and explained the Yakobson's paradox[26] on the scatterness of carbon nanotube thickness and Young's modulus resulting from the use of (20).

5. RESULTS FOR BORON-NITRIDE NANOTUBES

Following the same approach we have studied the single-wall BNNTs subject to uniaxial tension. Instead of presenting the Young's modulus E and thickness h which depend on the type of loading, we show their well-defined product Eh versus radius R in Figure 3 for armchair and zigzag

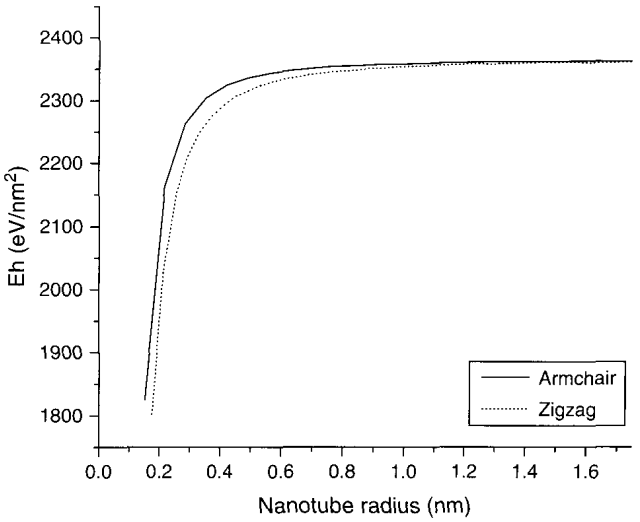

Fig. 3. The product of Young's modulus E and nanotube thickness h versus the nanotube radius R.

BNNTs. For $R>0.6$ nm, Eh is essentially independent of the nanotube radius and chirality, and is the same as its counterparts in (18) for the h-BN monolayer. Therefore, the tensile stiffness EA of a single-wall BNNT can be approximated by Eh in (18) multiplied by the perimeter of BNNT, i.e.,

$$(EA)_{\text{single-wall}}=Eh\cdot 2\pi R=\frac{\pi R}{2\sqrt{3}}\frac{\left(\frac{\partial^2 V}{\partial r_{ij}^2}\right)_0 B}{\left(\frac{\partial^2 V}{\partial r_{ij}^2}\right)_0+\frac{B}{8}} \tag{23}$$

The bending stiffness EI for a single-wall BNNT can be obtained from the thin shell model[25] with Young's modulus E and thickness h, i.e.,

$$(EI)_{\text{single-wall}}=Eh\cdot\pi R^3=\frac{\pi R^3}{4\sqrt{3}}\frac{\left(\frac{\partial^2 V}{\partial r_{ij}^2}\right)_0 B}{\left(\frac{\partial^2 V}{\partial r_{ij}^2}\right)_0+\frac{B}{8}} \tag{24}$$

The BNNT bending stiffness results from Eh, and is therefore very different from the bending stiffness $\sqrt{3}(\partial V/\partial\cos\theta_{ijk})_0/2$ for an h-BN monolayer which results from the multi-body atomistic interactions. In fact, the bending stiffness in (24) for a BNNT is much larger than the bending stiffness $\sqrt{3}(\partial V/\partial\cos\theta_{ijk})_0/2$ for an h-BN monolayer multiplied by the BNNT perimeter $2\pi R$. Their ratio is 144 for the (5,5) armchair BNNT and 572 for (10, 10) armchair BNNT using Albe et al.'s[16] potential.

For multi-wall BNNTs with radii $R_1, R_2, \ldots$ and R_n, the tensile stiffness is

$$(EA)_{\text{multi-wall}}=\frac{\pi}{2\sqrt{3}}(R_1+R_2+\cdots+R_n)\frac{\left(\frac{\partial^2 V}{\partial r_{ij}^2}\right)_0 B}{\left(\frac{\partial^2 V}{\partial r_{ij}^2}\right)_0+\frac{B}{8}} \tag{25}$$

where n is the number of walls. Similarly, the bending stiffness is given by

$$(EI)_{\text{multi-wall}} = \frac{\pi}{4\sqrt{3}}(R_1^3 + R_2^3 + \cdots + R_n^3)\frac{\left(\frac{\partial^2 V}{\partial r_{ij}^2}\right)_0 B}{\left(\frac{\partial^2 V}{\partial r_{ij}^2}\right)_0 + \frac{B}{8}} \quad (26)$$

Let d denote the equilibrium distance between BNNT walls, which is around 0.34 nm.[27,28] For van der waals interactions between nanotubes, Lu et al.[29] showed that the wall spacing d is the same as the equilibrium distance σ in the Lennard-Jones potential $U = 4\varepsilon[(\sigma/r)^{12} - (\sigma/r)^6]$. The inner most and outer most wall radii are then related by $R_{\text{out}} - R_{\text{in}} = (n-1)d$. Equations (25) and (26) then become

$$(EA)_{\text{multi-wall}} = \frac{n\pi}{2\sqrt{3}}\left(R_{\text{in}} + \frac{n-1}{2}d\right)\frac{\left(\frac{\partial^2 V}{\partial r_{ij}^2}\right)_0 B}{\left(\frac{\partial^2 V}{\partial r_{ij}^2}\right)_0 + \frac{B}{8}}$$

$$= \frac{n\pi}{2\sqrt{3}}\left(R_{\text{out}} - \frac{n-1}{2}d\right)\frac{\left(\frac{\partial^2 V}{\partial r_{ij}^2}\right)_0 B}{\left(\frac{\partial^2 V}{\partial r_{ij}^2}\right)_0 + \frac{B}{8}} \quad (27)$$

and

$$(EI)_{\text{multi-wall}} = \frac{n\pi R_{\text{in}}^3}{4\sqrt{3}}\left[1 + \frac{3(n-1)}{2}\frac{d}{R_{\text{in}}} + \frac{(n-1)(2n-1)}{2}\frac{d^2}{R_{\text{in}}^2} + \frac{n(n-1)^2}{4}\frac{d^3}{R_{\text{in}}^3}\right]\frac{\left(\frac{\partial^2 V}{\partial r_{ij}^2}\right)_0 B}{\left(\frac{\partial^2 V}{\partial r_{ij}^2}\right)_0 + \frac{B}{8}}$$

$$= \frac{n\pi R_{\text{out}}^3}{4\sqrt{3}}\left[1 - \frac{3(n-1)}{2}\frac{d}{R_{\text{out}}} + \frac{(n-1)(2n-1)}{2}\frac{d^2}{R_{\text{out}}^2} - \frac{n(n-1)^2}{4}\frac{d^3}{R_{\text{out}}^3}\right]\frac{\left(\frac{\partial^2 V}{\partial r_{ij}^2}\right)_0 B}{\left(\frac{\partial^2 V}{\partial r_{ij}^2}\right)_0 + \frac{B}{8}} \quad (28)$$

6. CONCLUDING REMARKS

The tensile and bending stiffness of a hexagonal boron-nitride (h-BN) monolayer are obtained *analytically* in terms of the parameters in the interatomic potential such that one can bypass molecular dynamics simulations to determine the stiffness directly. The h-BN monolayer thickness previously defined from the bending to tensile stiffness ratio is not a constant and depends on the type of loading. This conclusion also holds for boron-nitride nanotubes (BNNTs). The tensile and bending stiffness of single-wall and multi-wall BNNTs are also obtained *analytically* in terms of the interatomic potential, BNNT (inner most or outer most) radius, and the number of walls.

APPENDIX

The second-order derivatives in (3) can be *analytically* obtained for Albe et al.'s[16] potential as

$$\left(\frac{\partial^2 V}{\partial r_{ij}^2}\right)_0 = 2\beta^2 D_0 B_0^{\frac{S}{S-1}} \quad (A1)$$

$$\left(\frac{\partial^2 V}{\partial r_{ij}\partial\cos\theta_{ijk}}\right)_0 = \beta\frac{\sqrt{2S}D_0}{S-1}\gamma c^2\frac{(h^*+1/2)}{[d^2+(h^*+1/2)^2]^2} \times(2\gamma G_0)^{n-1}B_0^{2n+\frac{S}{S-1}} \quad (A2)$$

$$\left(\frac{\partial^2 V}{\partial\cos\theta_{ijk}\partial\cos\theta_{ijl}}\right)_0 \quad (k\neq l) = -\frac{SD_0}{S-1}\gamma^2 c^4\frac{(h^*+1/2)^2}{[d^2+(h^*+1/2)^2]^4} \times(2\gamma G_0)^{n-2}B_0^{4n+\frac{S}{S-1}}[3(2\gamma G_0)^n - 2(n-1)] \quad (A3)$$

$$\left(\frac{\partial^2 V}{\partial\cos\theta_{ijk}\partial\cos\theta_{ijk}}\right)_0 = \left(\frac{\partial^2 V}{\partial\cos\theta_{ijk}\partial\cos\theta_{ijl}}\right)_0 \quad (k\neq l) - \frac{SD_0}{S-1}\gamma c^2 \times\frac{3(h^*+1/2)^2 - d^2}{[d^2+(h^*+1/2)^2]^3}(2\gamma G_0)^{n-1}B_0^{2n+\frac{S}{S-1}} \quad (A4)$$

Acknowledgments: Y. Huang acknowledges the supports from the NSF through Nano-CEMMS (grant #DMI03-28162) at the University of Illinois and ONR Composites for Marine Structures Program (grant N00014-01-1-0205, Program Manager Dr. Y. D. S. Rajapakse). The authors also acknowledge the supports from the NSFC and Ministry of Education of China. K. C. Hwang also acknowledges the support from National Basic Research Program of China (973 Program) Grant No.2007CB936803.

References and Notes

1. E. Hernández, C. Goze, P. Bernier, and A. Rubio, *Phys. Rev. Lett.* 80, 4502 (**1998**).
2. E. Hernández, C. Goze, P. Bernier, and A. Rubio, *Appl. Phys. A* 68, 287 (**1999**).
3. K. N. Kudin, G. E. Scuseria, and B. I. Yakoboson, *Phys. Rev. B* 64, 235406 (**2001**).
4. C. W. Chang, W. Q. Han, and A. Zettl, *Appl. Phys. Lett.* 86, 173102 (**2005**).
5. X. Blase, A. Rubio, S. Louie, and M. Cohen, *Europhys. Lett.* 28, 335 (**1994**).
6. Y. Chen, J. Zou, S. Campbell, and G. Caer, *Appl. Phys. Lett.* 84, 2430 (**2004**).
7. N. G. Chopra and A. Zettl, *Solid State Commun.* 105, 297 (**1998**).
8. A. P. Suryavanshi, M. F. Yu, J. G. Wen, C. C. Tang, and Y. Bando, *Appl. Phys. Lett.* 84, 2527 (**2004**).
9. L. Vaccarini, C. Goze, L. Henrard, E. Hernández, P. Bernier, and A. Rubio, *Carbon* 38, 1681 (**2000**).
10. H. F. Bettinger, T. Dumitrică, G. E. Scuseria, and B. I. Yakobson, *Phys. Rev. B* 65, 041406 (**2002**).
11. B. Akdim, R. Pachter, X. F. Duan, and W. W. Adams, *Phys. Rev. B* 67, 245404 (**2003**).

12. T. Dumitrică, H. F. Bettinger, G. E. Scuseria, and B. I. Yakobson, *Phys. Rev. B* 68, 085412 (**2003**).
13. W. H. Moon and H. J. Hwang, *Nanotechnology* 15, 431 (**2004a**).
14. W. H. Moon and H. J. Hwang, *Phys. Lett. A* 320, 446 (**2004b**).
15. J. Song, Y. Huang, H. Jiang, K. C. Hwang, and M. F. Yu, *Int. J. Mech. Sci.* 48, 1197 (**2006**).
16. K. Albe, W. Möller, and K. H. Heinig, *Radiat. Eff. Defects Solids* 141, 85 (**1997a**).
17. K. Albe and W. Möller, *Comput. Mater. Sci.* 10, 111 (**1998**).
18. B. I. Yakobson, C. J. Brabec, and J. Bernholc, *Phys. Rev. Lett.* 76, 2511 (**1996**).
19. Y. Huang, J. Wu, and K. C. Hwang, *Phys. Rev. B* 74, 245413 (**2006**).
20. K. Albe, *Phys. Rev. B* 55, 6203 (**1997b**).
21. H. Koga, Y. Nakamura, S. Watanabe, and T. Yoshida, *Surf. Coat. Tech.* 142, 911 (**2001**).
22. G. J. Sibona, S. Schreiber, R. H. W. Hoppe, B. Stritzker, and A. Revnic, *Mat. Sci. Semicon. Proc.* 6, 71 (**2003**).
23. P. Zhang, Y. Huang, P. H. Geubelle, P. A. Klein, and K. C. Hwang, *Int. J. Solids Struct.* 39, 3893 (**2002**).
24. P. Zhang, Y. Huang, P. H. Geubelle, and K. C. Hwang, *J. Mech. Phys. Solids* 52, 977 (**2004**).
25. S. Timoshenko, Theory of Plates and Shells, McGraw-Hill, New York (**1940**).
26. O. A. Shenderova, D. W. Zhirnov, and D. W. Brenner, *Crit. Rev. Solid State* 27, 227 (**2002**).
27. A. Loiseau, F. Willaime, N. Demoncy, G. Hug, and H. Pascard, *Phys. Rev. Lett.* 76, 4737 (**1996**).
28. R. Ma, Y. Bando, T. Sato, and K. Kurashima, *Chem. Mater.* 13, 2965 (**2001**).
29. W. B. Lu, J. Wu, L. Y. Jiang, Y. Huang, K. C. Hwang, and B. Liu, *Philos. Mag.* 87, 2221 (**2007**).

Received: 23 January 2007. Accepted: 10 May 2007.

RESEARCH ARTICLE